



HAL
open science

Telomerase Repairs Collapsed Replication Forks at Telomeres

Samah Matmati, Sarah Lambert, Vincent Geli, Stephane Coulon

► **To cite this version:**

Samah Matmati, Sarah Lambert, Vincent Geli, Stephane Coulon. Telomerase Repairs Collapsed Replication Forks at Telomeres. *Cell Reports*, 2020, 30 (10), pp.3312 - 3322. 10.1016/j.celrep.2020.02.065 . hal-02505864

HAL Id: hal-02505864

<https://hal.science/hal-02505864>

Submitted on 11 Mar 2020

HAL is a multi-disciplinary open access archive for the deposit and dissemination of scientific research documents, whether they are published or not. The documents may come from teaching and research institutions in France or abroad, or from public or private research centers.

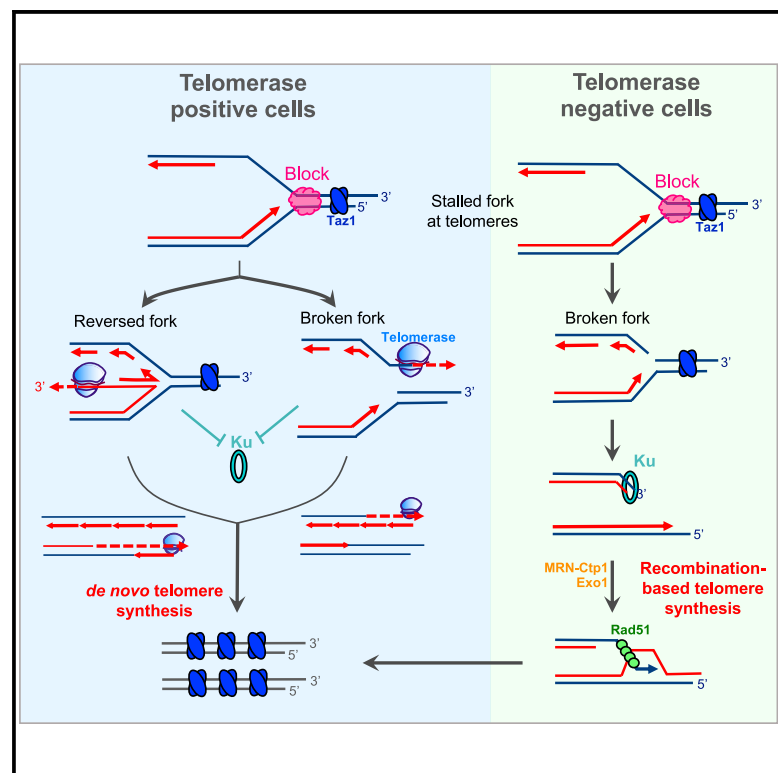
L'archive ouverte pluridisciplinaire **HAL**, est destinée au dépôt et à la diffusion de documents scientifiques de niveau recherche, publiés ou non, émanant des établissements d'enseignement et de recherche français ou étrangers, des laboratoires publics ou privés.



Distributed under a Creative Commons Attribution - NonCommercial - NoDerivatives 4.0 International License

Telomerase Repairs Collapsed Replication Forks at Telomeres

Graphical Abstract



Authors

Samah Matmati, Sarah Lambert,
Vincent Géli, Stéphane Coulon

Correspondence

vincent.geli@inserm.fr (V.G.),
stephane.coulon@inserm.fr (S.C.)

In Brief

Matmati et al. investigate replication dynamics in telomerase-negative fission yeast cells. Their results reveal that telomerase repairs collapsed replication forks at telomeres and shields telomeres from homologous recombination.

Highlights

- Telomerase repairs collapsed replication forks at telomeres
- Rad51, MRN, and Ctp1 are essential in the absence of telomerase
- Ku and Trt1 compete for telomeric free DNA ends



Telomerase Repairs Collapsed Replication Forks at Telomeres

Samah Matmati,¹ Sarah Lambert,^{2,3} Vincent Géli,^{1,*} and Stéphane Coulon^{1,4,*}

¹Marseille Cancer Research Centre (CRCM), U1068 INSERM, UMR7258 CNRS, UM105 Aix-Marseille University, Institut Paoli-Calmettes, Ligue Nationale Contre le Cancer (équipe labellisée) Marseille, F-13009, France

²Institut Curie, PSL Research University, CNRS, UMR3348, F-91405 Orsay, France

³University Paris Sud, Paris-Saclay University, CNRS, UMR3348, F-91405 Orsay, France

⁴Lead Contact

*Correspondence: vincent.geli@inserm.fr (V.G.), stephane.coulon@inserm.fr (S.C.)

<https://doi.org/10.1016/j.celrep.2020.02.065>

SUMMARY

Telomeres are difficult-to-replicate sites whereby replication itself may threaten telomere integrity. We investigate, in fission yeast, telomere replication dynamics in telomerase-negative cells to unmask problems associated with telomere replication. Two-dimensional gel analysis reveals that replication of telomeres is severely impaired and correlates with an accumulation of replication intermediates that arises from stalled and collapsed forks. In the absence of telomerase, Rad51, Mre11-Rad50-Nbs1 (MRN) complex, and its co-factor CtIP^{Ctp1} become critical to maintain telomeres, indicating that homologous recombination processes these intermediates to facilitate fork restart. We further show that a catalytically dead mutant of telomerase prevents Ku recruitment to telomeres, suggesting that telomerase and Ku both compete for the binding of telomeric-free DNA ends that are likely to originate from a reversed fork. We infer that Ku removal at collapsed telomeric forks allows telomerase to repair broken telomeres, thereby shielding telomeres from homologous recombination.

INTRODUCTION

Telomeres are nucleoprotein structures that protect chromosome extremities from degradation and ensure replication of chromosome ends (de Lange, 2018; Palm and de Lange, 2008). Telomeric DNA consists of repeated G-rich sequences that are gradually lost with the successive cellular divisions. In germinal and stem cells, telomere length is maintained by the activity of telomerase, a reverse transcriptase that is able to elongate the 3' overhang by addition of telomeric repeats. Telomeres are difficult regions to replicate and replication forks often stall when they progress through telomeric sequences (Sfeir et al., 2009). Indeed, several sources of endogenous stress impede replication fork progression such as telomeric DNA bound proteins, T-loops, RNA:DNA hybrids, and DNA secondary structures (for review, see Higa et al., 2017; Maestroni et al., 2017b). Thus, accurate replication of

chromosomal *termini* is a prerequisite for telomere homeostasis. To limit replication stress at telomeres, shelterin proteins TRF1 and TRF2 recruit and regulate the action of a number of helicases and nucleases (Vannier et al., 2012; Ye et al., 2010; Zimmermann et al., 2014). This underscores the importance of the telomeric proteins for telomere replication (Gilson and Géli, 2007).

The fission yeast *Schizosaccharomyces pombe* has a shelterin-like complex that includes Taz1^{TRF1-2}, Pot1, Rap1, Poz1, Tpz1^{TPP1}, and Ccq1 proteins (Dehé and Cooper, 2010; Moser and Nakamura, 2009). Telomerase that is composed of the catalytic subunit Trt1^{TERT}, the regulatory subunit Est1, and the TER1^{TERC} RNA is constitutively expressed in yeast and guarantees telomere homeostasis (Armstrong and Tomita, 2017). Rad3^{ATR}- and Tel1^{ATM}-dependent phosphorylation of Ccq1 promotes recruitment of telomerase to telomeres by promoting Ccq1-Est1 interaction (Moser et al., 2011; Webb and Zakian, 2012; Yamazaki et al., 2012). Telomerase recruitment occurs in S/G₂ phase transition concomitantly with telomere replication (Moser et al., 2009a). As in mammalian cells, the replication forks slow down in the proximity of telomeric repeats in fission yeast (Miller et al., 2006), and efficient replication is required for telomere maintenance (Chang et al., 2013; Moser et al., 2009b). Indeed, telomeric proteins such as Taz1 and the Stn1-Ten1 complex are known to promote efficient replication of telomeres (Matmati et al., 2018; Miller et al., 2006; Takikawa et al., 2017) as well as the RPA heterotrimer and Pfh1 helicase (Audry et al., 2015; Luciano et al., 2012; McDonald et al., 2014).

In fission yeast, deleting either of the protein subunits of telomerase or its RNA template leads to replicative senescence (Nakamura et al., 1998; Webb and Zakian, 2008). In the absence of telomerase activity, telomeres gradually shorten until the cells either cease dividing or die (crisis). This definitive arrest is caused by a DNA damage checkpoint that is activated as a result of unprotected short telomeres being recognized as irreparable double-strand breaks (DSBs). In *S. cerevisiae*, cell division capacity declines with time in the absence of telomerase activity due to the occurrence of stochastic events during replicative senescence that slow down or stop cell cycle (Churikov et al., 2016; 2014; Xu et al., 2015). This led us to investigate the replication dynamic in *S. pombe* cells lacking telomerase to unmask the replication stress occurring at telomeres (Simon et al., 2016). Our results indicate that telomerase repairs



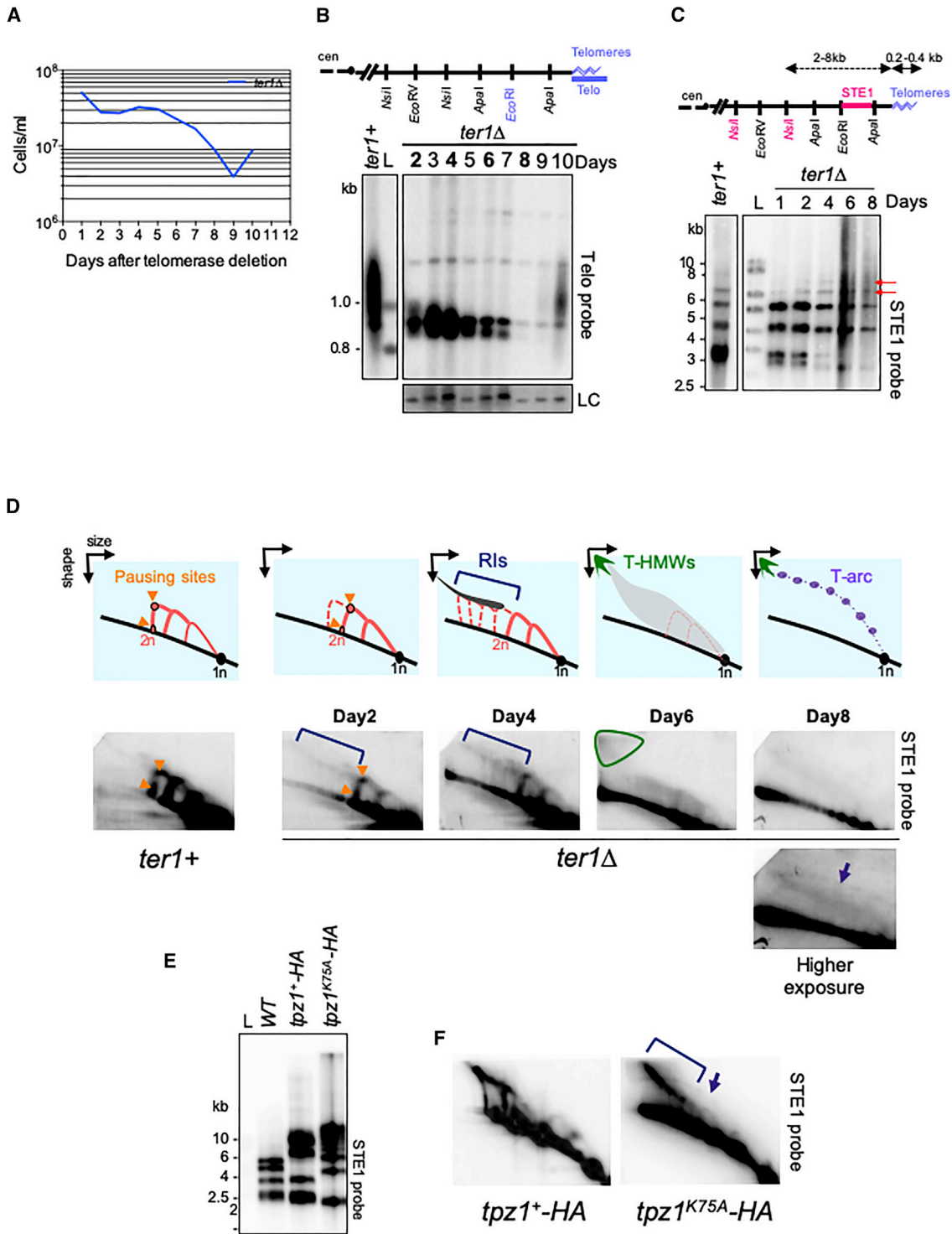


Figure 1. Replication Intermediates Accumulate at Telomeres in the Absence of Telomerase

(A) Representative replicative senescence profile of a freshly deleted *ter1Δ* clone propagated in liquid culture.

(B) Top: relative position of the restriction sites in the telomeric and subtelomeric regions of *S. pombe* chromosomes based on pNSU70 (cen, centromere). Telomeric probe (Telo) is represented by a blue bar. Bottom: genomic DNA from *ter1+* and *ter1Δ* cells was digested with *EcoRI* and Southern blotted. The membrane was hybridized with Telo probe that reveals telomeric signal. A chromosomal probe was used as a loading control (LC), and L corresponds to DNA ladder.

(legend continued on next page)

collapsed telomeric replication forks likely by binding to reversed fork.

RESULTS

Replication Intermediates Accumulate at Telomeres in the Absence of Telomerase

To investigate the replication dynamic at telomeres in cells lacking telomerase, we performed two-dimensional (2D) gel electrophoresis analysis as previously described (Audry et al., 2015; Miller et al., 2006). We performed replicative senescence kinetics (Webb and Zakian, 2008) by sampling daily dilutions of the liquid cultures established from the *ter1Δ* colonies. To ensure unique arrangement of the subtelomeric region, the *ter1Δ* colonies were obtained by transformation of a single parental strain (Figure 1A). In this representative experiment, crisis was reached after 9 days of growth corresponding to approximately 100–110 population doublings. Southern blot performed with a telomeric probe showed that crisis was concomitant with the disappearance of telomeric signal (Figure 1B). We next performed the first dimension of the 2D gel analysis of the *ter1+* and *ter1Δ* cells (Figure 1C). This Southern blot was revealed with a subtelomeric probe (STE1) to identify subtelomeric regions (*NsiI* pattern) of *S. pombe* strains allowing to predict 2D gel profile. In the *ter1+* parental strain *NsiI* digestion of genomic DNA released four telomere-containing restriction fragments from the six chromosome ends (Figure 1C, left panel), indicating that up to four Y-arcs might be detected after the second dimension. In telomerase-negative cells (*ter1Δ*), migration in the first dimension at different time points of the senescence showed that *NsiI* fragments faded with time and that additional high-molecular-weight bands and a smeared signal appeared (Figure 1C, right panel). This indicates that several additional replication intermediates (RIs) might be detected by the second dimension of *ter1Δ* samples. Migration in the second dimension of the *ter1+* sample revealed three Y-arcs containing strong pausing sites (Figure 1D, left panel). In agreement with the pattern observed in the first dimension, migration in the second dimension of the telomerase-negative samples revealed two Y-arcs at days 2 and 4 (Figure 1D). At day 4, the Y-arc signal slowly faded and spread into RIs of higher molecular complexity fragments that include Y-arcs like structures and likely X-shaped structures. At day 6, Y-arcs were barely visible, signal became fuzzy, and high-molecular-weight structures (HMWs) were detected, mimicking to some extent *taz1Δ* phenotype (Miller et al., 2006) (Figure 1D). At day 8, RIs were undistinguishable while a single telomeric arc (T-arc) was detectable as previously observed in *rpa1^{D223Y}* mutant reflecting severe replication defects (Audry et al., 2015). Another example

of a *ter1Δ* clone for which we analyzed in parallel the senescence profile and RIs by 2D gel is shown in Figure S1. Importantly, the appearance of these abnormal RIs correlated with the senescence profile, suggesting that the loss of growth capacity is related to replication defects that would be normally processed when telomerase is present.

To discriminate whether RIs accumulation resulted from a telomerase recruitment defect or telomere shortening, we monitored replication dynamics of the *tpz1^{K75A}* mutant that has short telomeres. Although the *tpz1^{K75A}* mutation lies in the TEL patch-like domain of Tpz1, it affects telomere elongation by telomerase rather than telomerase recruitment to telomeres (Armstrong et al., 2014). In the *tpz1+* parental strain (*tpz1-HA*), analysis of the *NsiI* pattern revealed multiple subtelomeric fragments that appeared as Y-arcs in the second dimension (Figures 1E and 1F). In the *tpz1^{K75A}* mutant, we observed a strong accumulation of additional RIs including HMWs and a T-arc that was barely visible (Figure 1F). This result suggests that telomere shortening per se induces a replication stress; however, this stress may also originate from the low processivity of telomerase in the *tpz1^{K75A}* mutant.

Finally, we wanted to determine whether the lack of the main DNA damage response kinase Rad3, which is also involved in telomerase recruitment, affects senescence profiles in telomerase-negative cells. The *rad3Δ trt1Δ* cells were obtained from tetrad dissection of the *rad3+/rad3Δ trt1+/trt1Δ* diploid strain that displayed wild-type telomere length (Figure S1D). As previously described (Nakamura et al., 2002), *rad3Δ trt1Δ* clones had a slow growth phenotype, and their senescence profiles were more heterogeneous than those of the *trt1Δ* clones (Figure S1E). Because of the slow growth phenotype of *rad3Δ trt1Δ* mutant, it was difficult to obtain a sufficient amount of cells to perform 2D gel analysis. To assess whether the absence of Trt1 activates a DNA damage response (DDR), we monitored checkpoint activation by following Chk1-myc and Cds1-myc phosphorylation in *trt1Δ* cells at different time points of the senescence (Figures S1F–S1H). Phosphorylation of Chk1 was detected only at time points of the senescence preceding the crisis, while phosphorylation of Cds1 was not observed. Taken together, these data indicate that telomere replication in the absence of telomerase does not activate the phosphorylation of these two kinases that act downstream of the Rad3 during canonical DDR.

Exo1 Processes Replication Intermediates at Telomeres

Homologous recombination (HR) requires Exo1-dependent DNA resection to promote homology search and strand invasion at DSBs (Langerak et al., 2011; Mimitou and Symington, 2008; Zhu et al., 2008). Recently, Exo1 was reported to also process

(C) Top: subtelomeric probe (STE1) is represented by a red bar. Subtelomeric fragments are heterogeneous in size. Bottom: Southern blot analysis of the telomeric *NsiI* fragments (first dimension) from the parental *ter1+* and *ter1Δ* cells revealed by STE1 probe. Red arrows mark additional subtelomeric fragments that appear during the time course of replicative senescence.

(D) 2D gel analysis of the telomeric *NsiI* fragments from the parental *ter1+* and *ter1Δ* cells revealed by STE1 probe. In second dimension, the Y-arc pattern is generated by unidirectional movement of a replication fork across each telomeric fragment seen in the first dimension. Orange triangles mark the strong pausing sites. In *ter1Δ* cells, abnormal replication intermediates (RIs) such as Y-arc-like structures and X-shaped molecules are depicted by brackets. High-molecular-weight structures (HMWs) (in green) and a telomeric arc (T-arc) (purple arrow) are detected at late time points during senescence.

(E) Southern blot analysis of the telomeric *NsiI* fragments (first dimension) from the parental *tpz1⁺-HA* and the *tpz1^{K75A}-HA* strains, revealed by STE1 probe.

(F) 2D gel analysis of *NsiI*-telomeric fragments revealed by STE1 probe. RIs, including HMWs (bracket) and T-arc (purple arrow), accumulate in *tpz1^{K75A}-HA* cells.

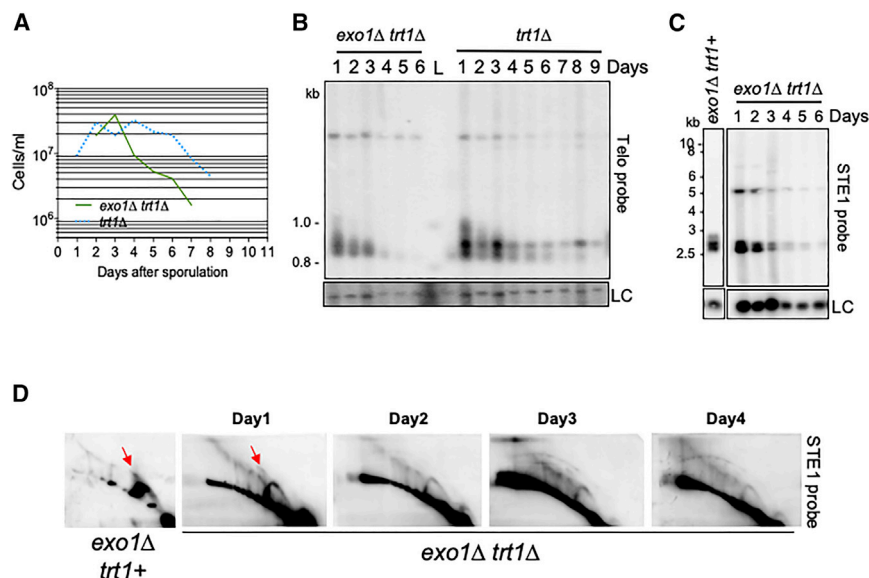


Figure 2. Exo1 Processes Replication Intermediates at Telomeres

(A) Representative replicative senescence profile of *exo1Δ trt1Δ* clone propagated in liquid culture. (B) Genomic DNA from *exo1Δ trt1Δ* cells was digested with *EcoRI* and Southern blotted. The membrane was hybridized with a Telo probe. A chromosomal probe was used as a loading control (LC). (C) Southern blot analysis of the telomeric *Nsil* fragments (first dimension) revealed by STE1 probe. (D) 2D gel analysis of the telomeric *Nsil* fragments revealed by STE1 probe. Y-arc like structures, X-shaped molecules, HMWs, and T-arcs accumulate in *exo1Δ trt1Δ* cells. Red arrows mark the cone-shaped signal (X-spike) that represents four-way DNA junctions emanating from Y-arc.

terminally arrested forks in *S. pombe* (Ait Saada et al., 2017). HR, as well as Ku, were both reported to restrain the Exo1-nucleolytic activity at arrested forks (Ait Saada et al., 2017; Teixeira-Silva et al., 2017). We thus examined the senescence profile and telomere RIs by 2D gel in the *exo1Δ trt1Δ* cells obtained from tetrad dissection of the *exo1+/exo1Δ trt1+/trt1Δ* diploid strain. In contrast to budding yeast in which deletion of *exo1* does not impair growth of telomerase minus cells (*est2Δ*) (Bertuch and Lundblad, 2004), we found that the absence of Exo1 accelerated senescence in *S. pombe* (crisis at day 7; Figure 2A) and resulted in the rapid loss of telomeres (Figure 2B), suggesting that Exo1 is required to support efficient telomere maintenance in the absence of telomerase.

In *exo1Δ trt1+* cells, analysis of *Nsil* pattern revealed three subtelomeric fragments of a similar size (Figure 2C, left panel) that appeared in the second dimension as a thick Y-arc with marked pausing sites (Figure 2D, left panel). X-shaped molecules emanated from the main pausing site and some RIs were also detected (red arrow). Although telomeres are mainly replicated as simple Y-arcs, these results indicate that Exo1 participates in telomere replication in telomerase-positive cells. In *exo1Δ trt1Δ* cells, telomere shortening occurred prematurely (Figure 2B). The *Nsil* pattern observed with *exo1Δ trt1Δ* clone in the first dimension is different from *exo1Δ trt1+* because *exo1Δ trt1Δ* clones were obtained from tetrad dissection of the *exo1+/exo1Δ trt1+/trt1Δ* diploid strain (Figure 2C). 2D gel analysis revealed numerous RIs with atypical appearance (Figure 2D). In the *exo1Δ trt1Δ* mutant, RIs were detected at earlier time points compared with the single *trt1Δ* mutant (Figure 1D). Remarkably, Y-arc like structures, X-shaped structures, HMWs, and T-arcs progressively accumulated with ongoing replicative senescence. We inferred from these results that Exo1 processes RIs, especially in the absence of telomerase. In *exo1Δ trt1Δ* cells, accumulation of RIs correlated with accelerated telomere shortening and senescence. These results support the hypothesis that telomerase promotes efficient replica-

tion of telomeres by preventing engagement of the telomeric RIs in HR.

Rad51, MRN, and Ctp1 Are Required to Sustain Cell Viability in the Absence of Telomerase

To investigate the roles of HR during telomeres replication in telomerase-negative cells, we constructed *trt1Δ/trt1+* diploid strain combined with either *rad51*, *mre11*, or *ctp1* deletions. Tetrad analysis revealed that the spores bearing *trt1Δ* and *rad51Δ* deletions were either synthetically lethal or extremely sick, preventing their propagation (Figure 3A). The same phenotype was observed when *trt1Δ* was associated with *rad51-III3A* (Figure 3B), a mutant of Rad51 that is able to form a stable nucleoprotein filament on single-stranded DNA (ssDNA) but unable to perform the strand-exchange reaction (Ait Saada et al., 2017). Chromatin immunoprecipitation (ChIP) experiments indicated that Rad51 was recruited to telomeres during replicative senescence (Figures 3C and S2), its binding being maximum at day 4 concomitantly with the visualization of Y-arcs-like structures, X-shaped molecules, and HMWs by 2D gel (Figure 1D). We concluded that Rad51 fulfills essential functions in the absence of telomerase, likely by processing RIs through strand-exchange reaction. Rad55 is known to assist Rad51 in the formation of the nucleoprotein filament. Although *trt1Δ rad55Δ* spore was viable, we were unable to further grow double mutants in liquid culture, thus confirming the essential role of HR in the absence of telomerase (Figure 3D).

MRN (Mre11-Rad50-Nbs1) complex and its co-factor Ctp1 are required for DSB repair by HR. MRN-Ctp1 have been proposed to release Ku from DNA ends and to initiate resection (Jensen and Russell, 2016; Langerak et al., 2011; Limbo et al., 2007). Tetrad analysis revealed that *mre11Δ trt1Δ* and *ctp1Δ trt1Δ* were synthetically lethal or sick (Figures 3E and 3F), showing that both are required in the absence of telomerase. When *trt1Δ* was combined with the *mre11-D65N* mutant that is deficient in nuclease activity but proficient in MRN complex formation (Hartsuiker et al., 2009), the double mutant was viable in

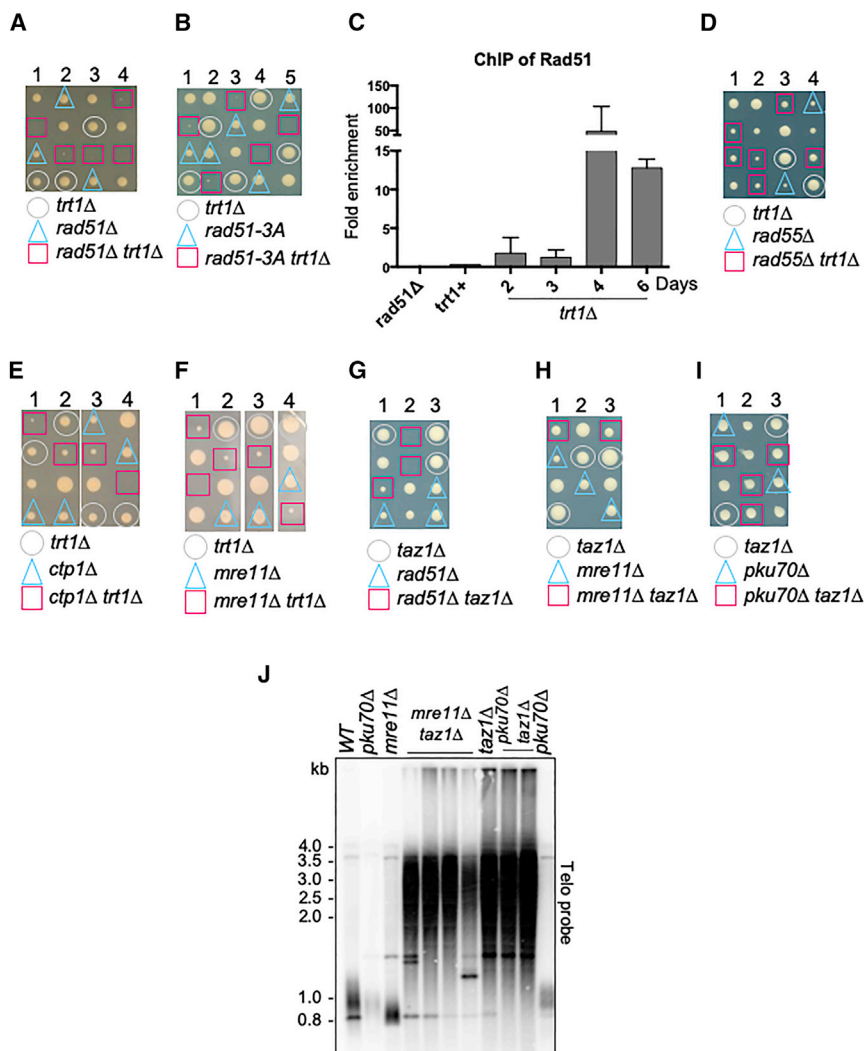


Figure 3. Rad51, Ctp1, and Mre11 Are Essential in the Absence of Telomerase

(A, B, and D–F) Analysis of spore viability resulting from tetrad dissection of a mating between *trt1Δ* and *rad51Δ*, *rad51-III3A*, *rad55Δ*, *ctp1Δ*, and *mre11Δ* mutants.

(C) ChIP of Rad51 at telomeres in untagged (*trt1+*), *rad51Δ*, and *trt1Δ* strains. The immunoprecipitated DNA was analyzed by quantitative PCR with the telomeric and chromosomal primers. Telomeric primers are located within STE1 subtelomeric region in close proximity to telomeric repeats. Data are the mean of two independent clones.

(G–I) Viability analysis of the spore colonies resulting from tetrad dissection after mating between *taz1Δ* and *rad51Δ*, *mre11Δ* and *pku70Δ* mutants. (J) Genomic DNA was digested with *EcoRI* and Southern blotted. The membrane was hybridized with Telo probe that reveals telomeric signal. A chromosomal probe was used as a loading control (LC), and L corresponds to DNA ladder.

contrast to the *mre11Δ trt1Δ* mutant (Figure S3A). Nevertheless, this mutation accelerated senescence since the crisis was reached at day 5 (Figure S3B), suggesting that both the nuclease activity of Mre11 and the structural function of MRN were required to maintain telomeres in the absence of telomerase. Taken together, these results show that Rad51, MRN, and Ctp1 are essential factors in telomerase minus cells that ensure telomere maintenance and sustain cell viability. Noteworthy, we observed that the Rad8 ubiquitin ligase/DNA helicase was dispensable for viability of telomerase-negative cells during senescence (Figures S3C and S3D), although its *S. cerevisiae* counterpart Rad5 has been shown to promote the viability of cells in the absence of telomerase (Fallet et al., 2014).

Taz1 is known to promote efficient replication of telomeric DNA (Miller et al., 2006). Indeed, Taz1 loss leads to stalled replication forks, and telomere maintenance in *taz1Δ* cells relies on the telomerase, which is recruited throughout the cell cycle (Dehé et al., 2012). Because *taz1Δ* cells accumulate RIs, we wondered how deletion of *rad51* and *mre11* would impact the viability of the double mutants. Like *rad51Δ trt1Δ*, the synthetic lethality (or sickness)

between *rad51Δ* and *taz1Δ* did not allow us to propagate *rad51Δ taz1Δ* cells (Figure 3G). In contrast, the absence of Mre11 neither impaired the growth of *taz1Δ* mutant (Figure 3H) nor its telomere maintenance (Figure 3J). Thus, while Rad51 is required to sustain viability in the absence of either Trt1 or Taz1, Mre11 is only required in the absence of Trt1, while it is dispensable in *taz1Δ* cells pointing out the specific role of Mre11 in telomerase-negative cells.

Ku and Trt1 Are Mutually Exclusive at Telomeric Free DNA Ends

Along the same lines, we observed that the deletion of *pku70* in the absence of

telomerase was deleterious for cell viability, although *pku70Δ trt1Δ* spores were able to form colonies (Figures 4A and 4B), consistent with previous observations (Baumann and Cech, 2000). Of note, this contrasts with the absence of genetic interaction between *taz1Δ* and *pku70Δ* (Figures 3I and 3J). ChIP experiments revealed that Ku70 was recruited at early time points of the replicative senescence (Figure 4C). Because it has been shown recently that Ku complex can load onto the terminally arrested forks that undergo reversal (Teixeira-Silva et al., 2017), we hypothesized that broken or reversed replication forks at telomeres may produce a substrate for Ku. We tested the possibility that Ku and telomerase compete for the binding of dsDNA ends. To this purpose, we took advantage of a catalytically dead (CD) mutant of telomerase (*trt1-D744A*; *trt1^{CD}*) (Haering et al., 2000). As previously described (Subramanian et al., 2008), we confirmed that this mutant rapidly loses its telomeres (Figures 4D and 4E). Indeed, *trt1^{CD}* cells obtained from *trt1+/trt1^{CD}* diploid strain reached crisis at day 5. By ChIP of Est1-V5, we verified that telomerase is recruited to telomeres as has been already shown (Subramanian et al., 2008) (Figures 4F and

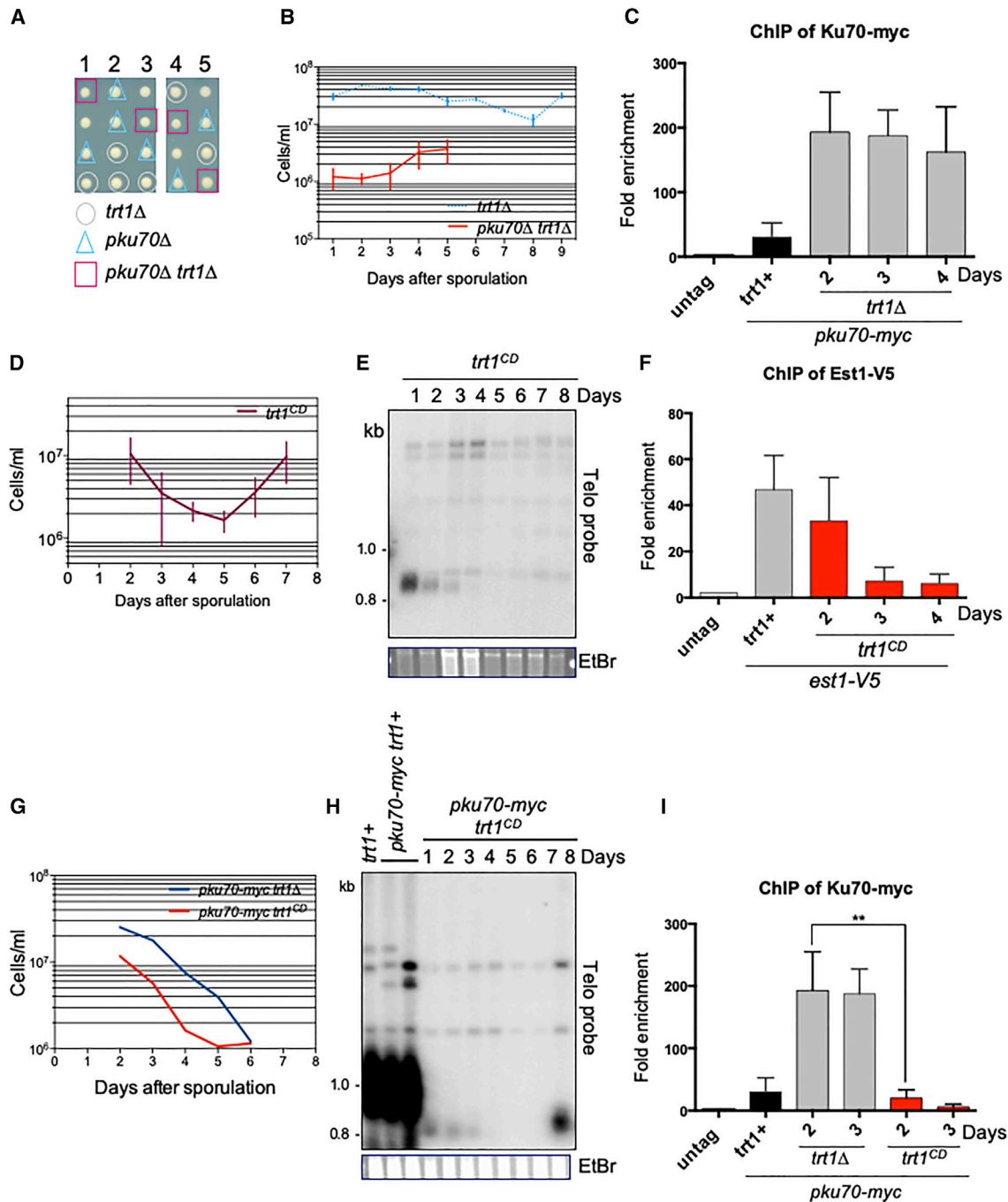


Figure 4. Telomerase Catalytically Dead Mutant Prevents Ku Binding at Telomeres

(A) Analysis of spore viability resulting from tetrad dissection of a mating between *trt1*Δ and *ku70*Δ mutants.

(B) Average replicative senescence profiles of the *pku70*Δ *trt1*Δ (n = 4) and of the *trt1*Δ (n = 5) clones (latter being obtained by sporulation of the *trt1*+/*trt1*Δ diploid) propagated in liquid culture.

(C, F, and I) ChIP of the Est1-V5 and Ku70-myc at telomeres in untagged, *trt1*+, *trt1*Δ, and *trt1*^{CD} strains. The immunoprecipitated DNA was analyzed by quantitative PCR using the telomeric and chromosomal primers as explained in the legend to Figure 3C. Data are the mean of three independent experiments.

(D) Replicative senescence profile of the catalytically dead telomerase (*trt1*^{CD}) clones (n = 3) propagated in liquid culture, obtained after sporulation of the *trt1*^{CD} *trt1*Δ diploid strain.

(E and H) Genomic DNA from the indicated strains was digested with *Eco*RI and Southern blotted. The membrane was hybridized with a Telo probe. Ethidium bromide staining was used as a loading control (EtBr).

(G) Representative replicative senescence profile of the *pku70-myc trt1*Δ and *pku70-myc trt1*^{CD} clones propagated in liquid culture.

S4A–S4C). Indeed, Est1-V5 binding was detected at day 2 of the replicative senescence, and later ChIP signal decreased concomitantly with the loss of telomeric signal. These results show that the catalytically dead telomerase accelerates the rate of senescence and telomere loss compared to *trt1* deletion.

Next, we performed ChIP of Ku70-myc protein in *trt1* Δ and *trt1*^{CD} genetic backgrounds. We confirmed that senescence was accelerated in *ku70-myc trt1*^{CD} compared to *ku70-myc trt1* Δ as reported above (Figures 4G and 4H). *trt1*^{CD} and *ku70-myc trt1*^{CD} mutants exhibited similar senescence and telomere shortening kinetics, indicating that the tagged version of Ku70 did not affect the senescence profile of the *trt1*^{CD} mutant (compare Figures 4D and 4G). Strikingly, the Trt1^{CD} prevented the recruitment of Ku70 at telomeres (Figure 4I). The fact that the recruitment of Ku70 is impaired by the Trt1^{CD} suggests that both proteins compete for the same substrate at telomeres, likely for the telomeric free DNA ends formed at either broken or reversed forks. In support of this hypothesis, we found that recruitment of Est1 at telomeres is increased in *ku70* Δ cells (Figure S4D). Conversely, Ku70 binding is not significantly increased in *taz1* Δ mutant that exhibits a high level of telomerase at chromosome ends (Figure S4E).

Importantly, *trt1+*/*trt1*^{CD} diploid cells had shorter telomeres than *trt1+*/*trt1* Δ cells indicating that Trt1^{CD} has a dominant-negative effect (Figure S5A), consistent with the fact that telomerase may act as a dimer (Wenz et al., 2001). To confirm that accelerated senescence was caused by the recruitment of an inactive form of telomerase in *trt1*^{CD} cells and not by short telomeres inherited from the parental *trt1+*/*trt1*^{CD} diploid strain, we transformed *trt1*^{CD} haploid cells with pTrt1+ plasmid that overexpresses Trt1 (pREP2-Trt1). This plasmid allowed to maintain telomeres of *trt1*^{CD} cells at a wild-type length (Figure S5A). Loss of pTrt1+ triggered an early onset in senescence of the *trt1*^{CD} cells (compared to *trt1* Δ cells) as crisis was reached at day 7 (Figure S5B). Accordingly, Southern blot confirmed a rapid loss of telomeric sequences in *trt1*^{CD} albeit it was delayed compared to *trt1*^{CD} obtained from sporulation of *trt1+*/*trt1*^{CD} (Figure S5C). This confirmed that the catalytically dead telomerase aggravates the senescence compared to the *trt1* deletion.

X-Shaped Molecules Accumulate in *trt1*^{CD}

When replication forks stall, they may also reverse (Teixeira-Silva et al., 2017). Since reversal within telomeric sequences is predicted to create a four-way branched structure (also called chicken foot) with a 3' overhang on the regressed double-strand end, telomerase can theoretically bind to this structure as it was previously proposed in *taz1* Δ cells (Dehé et al., 2012). With this hypothesis in mind, we monitored by 2D gel replication dynamics in *trt1*^{CD} cells obtained after loss of the pTrt1+ plasmid (Figures 5A and 5B). In the first dimension, we visualized a unique *NsiI* fragment that was converted into a single Y-arc in the second dimension (Figures 5C and 5D). Interestingly, we observed the accumulation of X-shaped molecules visible as a cone signal emanating from strong pausing site on the Y-arc (marked with a red arrow). Given that fork convergence does not occur at telomeres that are replicated by unidirectional forks, these data likely indicate that, in *trt1*^{CD} background, reversed replication forks are stabilized at telomeres. Noteworthy, X-spike emanating

from Y-arc was also visible in *exo1* Δ background (Figure 2D) and barely detectable in *trt1+* cells (Figure 1D). Although 2D gel cannot identify reversed forks unambiguously (Neelsen and Lopes, 2015), our data indicate that reversed replication forks are natural transient structures at telomeres. Taking together, these results suggest that telomerase can bind to either broken or reversed forks to complete their replication.

DISCUSSION

Replication forks naturally stall when they approach chromosome ends because of endogenous obstacles to fork progression such as telomeric DNA bound proteins, RNA:DNA hybrids, and DNA secondary structures. In this study, we present several pieces of evidence that telomerase is the preferred pathway for healing telomeres when the replication forks are stalled. Although 2D gel cannot identify reversed forks unambiguously, our results suggested that four-branch DNA structures emanate from stalled forks at telomeres. Thus, we propose that stalled forks do collapse and then either break or reverse, exposing G-rich single strand, which could be extended by telomerase, allowing *de novo* telomere synthesis (Figure 5E). Our findings are in line with the models proposed in budding (Simon et al., 2016) and fission yeast (Dehé et al., 2012), suggesting that telomerase acts as a repair enzyme at broken telomeres.

More recently, the binding of telomerase to reversed replication forks has been proposed in mouse RTEL1-deficient cell lines (Margalef et al., 2018). In this genetic context, telomerase inappropriately binds to and stabilizes reversed replication forks, thereby preventing replication fork restart. Here, we report that in fission yeast telomerase is able to extend the 3' end G-rich ssDNA at a reversed fork, thereby completing telomere replication. Telomerase would be detrimental only if it is catalytically inactive likely by hampering fork restart in a similar way as does mouse wild-type telomerase in RTEL1-deficient cells. Thus, in contrast to chromosomal DSBs, where telomere healing might lead to loss of genetic information, we might consider that telomerase acts as a repair enzyme of reversed or broken forks at telomeres. This would allow cells to maintain their telomeres through a HR-independent pathway. We explain the seeming contradiction between our results and those of Margalef et al. (2018) by the great difference in telomere length between mice and fission yeast. Mouse telomerase, particularly in the absence of RTEL1, would not be able to complete the synthesis of the many kilobases of telomeric DNA. It remains to be seen whether human telomerase is able to heal telomeres when replication forks collapse.

In this study, we also showed that Rad51, Ku, Mre11, Ctp1, and to a less extent Exo1 are required to sustain cell viability of *S. pombe* cells lacking telomerase activity (Figure 5E). In budding yeast, Rad51 is also essential in cells lacking telomerase (Churikov et al., 2014; Fallet et al., 2014; Nugent et al., 1998). However, in contrast to *S. pombe*, inactivation of either Mre11, Sae2^(Ctp1), or Exo1 in *S. cerevisiae* delays the onset of senescence (Ballew and Lundblad, 2013; Bertuch and Lundblad, 2004; Fallet et al., 2014; Hardy et al., 2014; Joseph et al., 2010; Nugent et al., 1998). These results suggest that the processing of collapsed forks at telomeres is likely different in *S. pombe* and *S. cerevisiae*. In budding yeast, the absence of the MRX complex and Exo1 decreases the

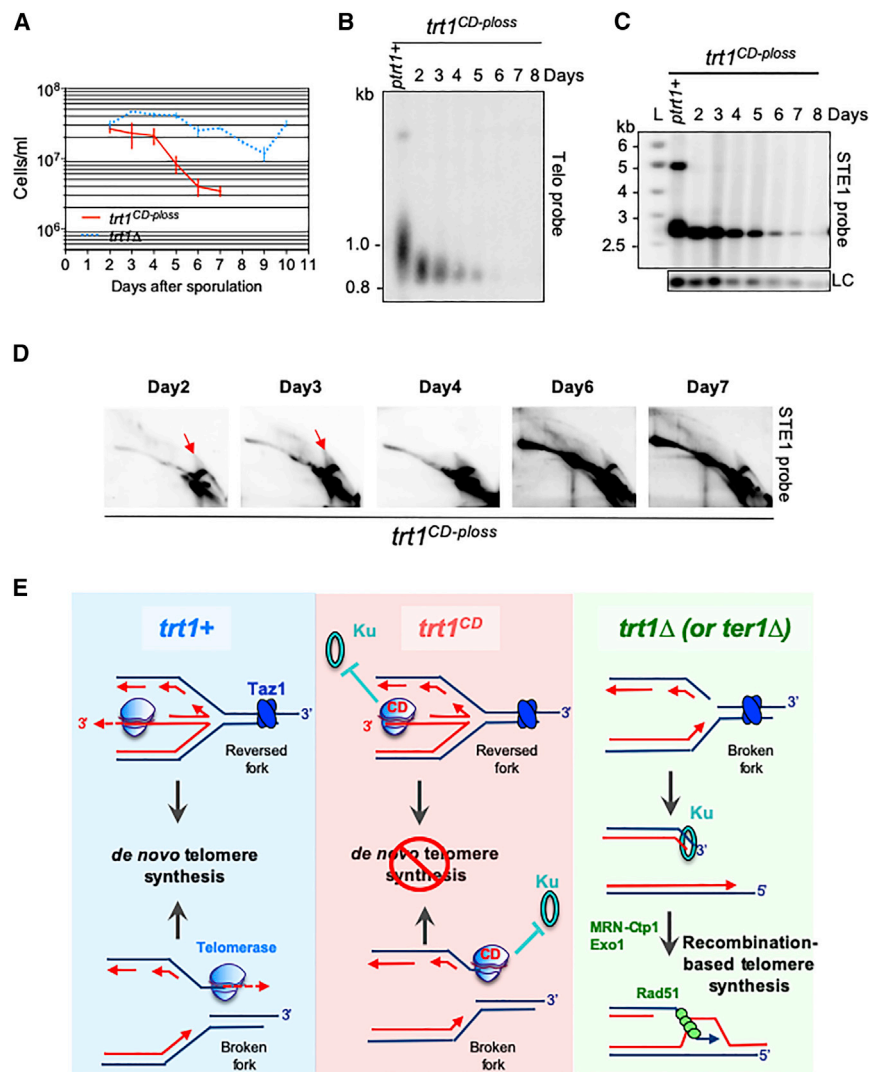


Figure 5. X-Shaped Molecules Accumulate in *trt1^{CD}*

(A) Replicative senescence profile of the *trt1^{CD}* strains issued from the pTrt1+ plasmid loss (*trt1^{CD-ploss}*; n = 3, red line). Blue dashed line corresponds to the *trt1Δ* (n = 5) clones obtained by sporulation of the *trt1+/trt1Δ* diploid. Senescence is accelerated in *trt1^{CD-ploss}* when compared to the *trt1Δ* cells.

(B) Telomere length analysis of *trt1^{CD-ploss}* strain issued from the pTrt1+ plasmid loss.

(C) Southern blot analysis of the telomeric *Nsil* fragments (first dimension) from *trt1^{CD-ploss}*. A chromosomal probe was used as a loading control (LC) (L, DNA ladder).

(D) 2D gel analysis of the telomeric *Nsil* fragments revealed by STE1 probe in *trt1^{CD-ploss}*. Red arrows mark the cone-shaped signal (X-spike) that represents four-way DNA junctions emanating from Y-arc at the pausing site.

(E) Model of the telomerase action at collapsed replication forks at telomeres. Replication forks naturally stall when they approach chromosome ends due to endogenous obstacles. Stalled forks may collapse and either break or reverse, exposing G-rich single strand, which can be further extended by telomerase to complete *de novo* telomere synthesis. The catalytically dead mutant of telomerase (Trt1^{CD}) is deleterious for the cells. We propose that Trt1^{CD} binds to the G-rich 3' overhangs but is unable to elongate telomeres. Occupancy of the reversed fork by Trt1^{CD} prevents recruitment of the Ku complex. In the absence of telomerase, the Ku complex, MRN-Ctp1, and HR pathway are essential for processing the collapsed forks. In this context, Ku may bind to the broken telomere and MRN-Ctp1 likely clips Ku and initiates resection that also requires Exo1. Then, Rad51-dependent HR repairs broken forks through a recombination-based repair mechanism.

extensive resection at critically short telomeres while in fission yeast the homologous factors play a role in the repair of the telomeric collapsed forks as does Rad51. Along the same lines, we found that Rad8 ubiquitin ligase/DNA helicase that belongs to the DNA damage tolerance pathway does not impact senescence in fission yeast, while its Rad5 homolog is necessary for telomere maintenance in *S. cerevisiae* (Fallet et al., 2014), accentuating the notion that budding and fission yeasts differently process replication stress at telomeres.

The use of the RTS1-blocked fork system in fission yeast has proposed that terminally arrested forks undergo fork reversal, providing a free DNA end for Ku binding (Teixeira-Silva et al., 2017). Indeed, the association of Ku with and its removal from reversed forks control end resection and replication fork restart mediated by HR. It is likely that the forks arrested at RTS1 and at telomeres share common restart mechanisms. Indeed, in this study, we show that Ku is recruited at telomeres in the absence of telomerase (Figure 5E), consistent with a recruitment of Ku at sites distal to chromosome ends as previously reported

in budding yeast (Larcher et al., 2016). In addition, we have shown that the presence of a catalytically dead mutant of telomerase prevents Ku binding suggesting that both proteins compete for the binding of free G-rich DNA ends at reversed forks (Figure 5E). While telomerase recruitment channels telomere repair by *de novo* telomere synthesis, Ku binding controls end resection and HR-mediated replication fork restart. This also implies that telomerase protects against telomere recombination by acting as a repair enzyme of the reversed forks.

In this study, we show that abnormal RIs appear immediately after removal of telomerase activity and accumulate with telomere shortening, indicating that the absence of telomerase generates replication stress (Figure 1D). Interestingly, replicative stress is also detected at short telomeres in the *tpz1^{K75A}* mutant in which telomerase does not efficiently elongate telomeres but remains recruited to chromosome ends (Figure 1F). The question arises whether short telomeres per se also contribute to replicative stress. Intuitively, it should be easier to replicate short telomeres than the longer ones since the amount of bound proteins

and secondary structures are supposed to be reduced. Therefore, we may wonder what the source of endogenous stress at short telomeres is. In budding and fission yeast, telomeric transcription is enhanced when telomeres shorten (Balk et al., 2013; Graf et al., 2017; Maestroni et al., 2017a; Moravec et al., 2016). Thus, the higher level of TERRA may provoke a replication stress at eroded telomeres that likely leads to the accumulation of RIs during replicative senescence. In addition, telomeric R-loops are thought to promote recombination-based telomere maintenance (Balk et al., 2013; Hu et al., 2019). Collectively, these data suggest that telomere shortening likely generates transcription-dependent replication stress and that both telomerase and HR contribute to the resolution of this replication stress (Figure 5E).

In summary, replication forks naturally slow down and stall at telomeres (Ivessa et al., 2002; Miller et al., 2006; Sfeir et al., 2009). When fork progression is stopped, it may reverse or break (Neelsen and Lopes, 2015). Fork reversal may stabilize the stalled fork and provide a G-rich single-strand DNA allowing telomerase recruitment and telomere maintenance.

STAR★METHODS

Detailed methods are provided in the online version of this paper and include the following:

- KEY RESOURCES TABLE
- LEAD CONTACT AND MATERIALS AVAILABILITY
- EXPERIMENTAL MODEL AND SUBJECT DETAILS
- METHOD DETAILS
 - Strains and Plasmids
 - Liquid senescence assay
 - Telomere length analysis by Southern blotting
 - Chromatin Immunoprecipitation (ChIP)
 - Two-dimensional (2D) gel electrophoresis
 - Protein extraction and western blots
- QUANTIFICATION AND STATISTICAL ANALYSIS
- DATA AND CODE AVAILABILITY

SUPPLEMENTAL INFORMATION

Supplemental Information can be found online at <https://doi.org/10.1016/j.celrep.2020.02.065>.

ACKNOWLEDGMENTS

We thank T. Nakamura, M.G. Ferreira, B. Arcangioli, K. Tomita, and J. Cooper for sharing strains and plasmids. We are grateful to A. Ait-Saada for sharing 2D gel protocols and to Dmitri Churikov for reading the manuscript and for critical comments. We also thank Marie-Noëlle Simon and the members of the V.G. team for helpful discussions. V.G.'s laboratory is supported by Ligue Nationale Contre le Cancer (LNCC) (équipe labélisée), and S.M. is supported by the LNCC. S.C. is supported by Projet Fondation ARC and by the Agence Nationale de la Recherche (ANR-16-CE12 TeloMito). S.L. is supported by Fondation pour la Recherche Médicale (Grant Equipe FRM DEQ20160334889).

AUTHOR CONTRIBUTIONS

S.M. performed the experiments. S.M., V.G., and S.C. designed experiments and analyzed the data. S.L. provided technical assistance and expertise in performing and analyzing 2D gel experiments. S.C. and V.G. wrote the paper.

DECLARATION OF INTERESTS

The authors declare no competing interests.

Received: September 17, 2019

Revised: January 17, 2020

Accepted: February 14, 2020

Published: March 10, 2020

REFERENCES

- Ait Saada, A., Teixeira-Silva, A., Iraqui, I., Costes, A., Hardy, J., Paoletti, G., Fréon, K., and Lambert, S.A.E. (2017). Unprotected replication forks are converted into mitotic sister chromatid bridges. *Mol. Cell* 66, 398–410.e4.
- Armstrong, C.A., and Tomita, K. (2017). Fundamental mechanisms of telomerase action in yeasts and mammals: understanding telomeres and telomerase in cancer cells. *Open Biol.* 7, 160338.
- Armstrong, C.A., Pearson, S.R., Amelina, H., Moiseeva, V., and Tomita, K. (2014). Telomerase activation after recruitment in fission yeast. *Curr. Biol.* 24, 2006–2011.
- Audry, J., Maestroni, L., Delagoutte, E., Gauthier, T., Nakamura, T.M., Gachet, Y., Saintomé, C., Géli, V., and Coulon, S. (2015). RPA prevents G-rich structure formation at lagging-strand telomeres to allow maintenance of chromosome ends. *EMBO J.* 34, 1942–1958.
- Balk, B., Maicher, A., Dees, M., Klermund, J., Luke-Glaser, S., Bender, K., and Luke, B. (2013). Telomeric RNA-DNA hybrids affect telomere-length dynamics and senescence. *Nat. Struct. Mol. Biol.* 20, 1199–1205.
- Ballew, B.J., and Lundblad, V. (2013). Multiple genetic pathways regulate replicative senescence in telomerase-deficient yeast. *Aging Cell* 12, 719–727.
- Baumann, P., and Cech, T.R. (2000). Protection of telomeres by the Ku protein in fission yeast. *Mol. Biol. Cell* 11, 3265–3275.
- Bertuch, A.A., and Lundblad, V. (2004). EXO1 contributes to telomere maintenance in both telomerase-proficient and telomerase-deficient *Saccharomyces cerevisiae*. *Genetics* 166, 1651–1659.
- Brewer, B.J., Lockshon, D., and Fangman, W.L. (1992). The arrest of replication forks in the rDNA of yeast occurs independently of transcription. *Cell* 71, 267–276.
- Chang, Y.-T., Moser, B.A., and Nakamura, T.M. (2013). Fission yeast shelterin regulates DNA polymerases and Rad3(ATR) kinase to limit telomere extension. *PLoS Genet.* 9, e1003936.
- Churikov, D., Charifi, F., Simon, M.N., and Géli, V. (2014). Rad59-facilitated acquisition of Y' elements by short telomeres delays the onset of senescence. *PLoS Genet.* 10, e1004736.
- Churikov, D., Charifi, F., Eckert-Boulet, N., Silva, S., Simon, M.N., Lisby, M., and Géli, V. (2016). SUMO-dependent relocalization of eroded telomeres to nuclear pore complexes controls telomere recombination. *Cell Rep.* 15, 1242–1253.
- de Lange, T. (2018). Shelterin-mediated telomere protection. *Annu. Rev. Genet.* 52, 223–247.
- Dehé, P.-M., and Cooper, J.P. (2010). Fission yeast telomeres forecast the end of the crisis. *FEBS Lett.* 584, 3725–3733.
- Dehé, P.-M., Rog, O., Ferreira, M.G., Greenwood, J., and Cooper, J.P. (2012). Taz1 enforces cell-cycle regulation of telomere synthesis. *Mol. Cell* 46, 797–808.
- Fallet, E., Jolivet, P., Soudet, J., Lisby, M., Gilson, E., and Teixeira, M.T. (2014). Length-dependent processing of telomeres in the absence of telomerase. *Nucleic Acids Res.* 42, 3648–3665.
- Gilson, E., and Géli, V. (2007). How telomeres are replicated. *Nat. Rev. Mol. Cell Biol.* 8, 825–838.
- Graf, M., Bonetti, D., Lockhart, A., Serhal, K., Kellner, V., Maicher, A., Jolivet, P., Teixeira, M.T., and Luke, B. (2017). Telomere length determines TERRA and R-loop regulation through the cell cycle. *Cell* 170, 72–85.e14.

- Haering, C.H., Nakamura, T.M., Baumann, P., and Cech, T.R. (2000). Analysis of telomerase catalytic subunit mutants in vivo and in vitro in *Schizosaccharomyces pombe*. *Proc. Natl. Acad. Sci. USA* 97, 6367–6372.
- Hardy, J., Churikov, D., Géli, V., and Simon, M.N. (2014). Sgs1 and Sae2 promote telomere replication by limiting accumulation of ssDNA. *Nat. Commun.* 5, 5004.
- Hartsuiker, E., Neale, M.J., and Carr, A.M. (2009). Distinct requirements for the Rad32(Mre11) nuclease and Ctp1(CtIP) in the removal of covalently bound topoisomerase I and II from DNA. *Mol. Cell* 33, 117–123.
- Higa, M., Fujita, M., and Yoshida, K. (2017). DNA replication origins and fork progression at mammalian telomeres. *Genes (Basel)* 8, E112.
- Hu, Y., Bennett, H.W., Liu, N., Moravec, M., Williams, J.F., Azzalin, C.M., and King, M.C. (2019). RNA-DNA hybrids support recombination-based telomere maintenance in fission yeast. *Genetics* 213, 431–447.
- Ivessa, A.S., Zhou, J.-Q., Schulz, V.P., Monson, E.K., and Zakian, V.A. (2002). *Saccharomyces Rrm3p*, a 5' to 3' DNA helicase that promotes replication fork progression through telomeric and subtelomeric DNA. *Genes Dev.* 16, 1383–1396.
- Jensen, K.L., and Russell, P. (2016). Ctp1-dependent clipping and resection of DNA double-strand breaks by Mre11 endonuclease complex are not genetically separable. *Nucleic Acids Res.* 44, 8241–8249.
- Joseph, I.S., Kumari, A., Bhattacharyya, M.K., Gao, H., Li, B., and Lustig, A.J. (2010). An mre11 mutation that promotes telomere recombination and an efficient bypass of senescence. *Genetics* 185, 761–770.
- Lambert, S., Mizuno, K., Blaisonneau, J., Martineau, S., Chanet, R., Fréon, K., Murray, J.M., Carr, A.M., and Baldacci, G. (2010). Homologous recombination restarts blocked replication forks at the expense of genome rearrangements by template exchange. *Mol. Cell* 39, 346–359.
- Langerak, P., Mejia-Ramirez, E., Limbo, O., and Russell, P. (2011). Release of Ku and MRN from DNA ends by Mre11 nuclease activity and Ctp1 is required for homologous recombination repair of double-strand breaks. *PLoS Genet.* 7, e1002271.
- Larcher, M.V., Pasquier, E., MacDonald, R.S., and Wellinger, R.J. (2016). Ku binding on telomeres occurs at sites distal from the physical chromosome ends. *PLoS Genet.* 12, e1006479.
- Limbo, O., Chahwan, C., Yamada, Y., de Bruin, R.A.M., Wittenberg, C., and Russell, P. (2007). Ctp1 is a cell-cycle-regulated protein that functions with Mre11 complex to control double-strand break repair by homologous recombination. *Mol. Cell* 28, 134–146.
- Luciano, P., Coulon, S., Faure, V., Corda, Y., Bos, J., Brill, S.J., Gilson, E., Simon, M.N., and Géli, V. (2012). RPA facilitates telomerase activity at chromosome ends in budding and fission yeasts. *EMBO J.* 31, 2034–2046.
- Maestroni, L., Audry, J., Matmati, S., Arcangioli, B., Géli, V., and Coulon, S. (2017a). Eroded telomeres are rearranged in quiescent fission yeast cells through duplications of subtelomeric sequences. *Nat. Commun.* 8, 1684.
- Maestroni, L., Matmati, S., and Coulon, S. (2017b). Solving the telomere replication problem. *Genes (Basel)* 8, 55.
- Margalef, P., Kotsantis, P., Borel, V., Bellelli, R., Panier, S., and Boulton, S.J. (2018). Stabilization of reversed replication forks by telomerase drives telomere catastrophe. *Cell* 172, 439–453.e14.
- Matmati, S., Vaurs, M., Escandell, J.M., Maestroni, L., Nakamura, T.M., Ferreira, M.G., Géli, V., and Coulon, S. (2018). The fission yeast Stn1-Ten1 complex limits telomerase activity via its SUMO-interacting motif and promotes telomeres replication. *Sci. Adv* 4, eaar2740.
- McDonald, K.R., Sabouri, N., Webb, C.J., and Zakian, V.A. (2014). The Pif1 family helicase Pfh1 facilitates telomere replication and has an RPA-dependent role during telomere lengthening. *DNA Repair (Amst.)* 24, 80–86.
- Miller, K.M., Rog, O., and Cooper, J.P. (2006). Semi-conservative DNA replication through telomeres requires Taz1. *Nature* 440, 824–828.
- Mimitou, E.P., and Symington, L.S. (2008). Sae2, Exo1 and Sgs1 collaborate in DNA double-strand break processing. *Nature* 455, 770–774.
- Moravec, M., Wischniewski, H., Bah, A., Hu, Y., Liu, N., Lafranchi, L., King, M.C., and Azzalin, C.M. (2016). TERRA promotes telomerase-mediated telomere elongation in *Schizosaccharomyces pombe*. *EMBO Rep.* 17, 999–1012.
- Moser, B.A., and Nakamura, T.M. (2009). Protection and replication of telomeres in fission yeast. *Biochem. Cell Biol.* 87, 747–758.
- Moser, B.A., Subramanian, L., Chang, Y.-T., Noguchi, C., Noguchi, E., and Nakamura, T.M. (2009a). Differential arrival of leading and lagging strand DNA polymerases at fission yeast telomeres. *EMBO J.* 28, 810–820.
- Moser, B.A., Subramanian, L., Khair, L., Chang, Y.-T., and Nakamura, T.M. (2009b). Fission yeast Tel1(ATM) and Rad3(ATR) promote telomere protection and telomerase recruitment. *PLoS Genet.* 5, e1000622.
- Moser, B.A., Chang, Y.-T., Kosti, J., and Nakamura, T.M. (2011). Tel1ATM and Rad3ATR kinases promote Ccq1-Est1 interaction to maintain telomeres in fission yeast. *Nat. Struct. Mol. Biol.* 18, 1408–1413.
- Nakamura, T.M., Cooper, J.P., and Cech, T.R. (1998). Two modes of survival of fission yeast without telomerase. *Science* 282, 493–496.
- Nakamura, T.M., Moser, B.A., and Russell, P. (2002). Telomere binding of checkpoint sensor and DNA repair proteins contributes to maintenance of functional fission yeast telomeres. *Genetics* 161, 1437–1452.
- Neelsen, K.J., and Lopes, M. (2015). Replication fork reversal in eukaryotes: from dead end to dynamic response. *Nat. Rev. Mol. Cell Biol.* 16, 207–220.
- Nugent, C.I., Bosco, G., Ross, L.O., Evans, S.K., Salinger, A.P., Moore, J.K., Haber, J.E., and Lundblad, V. (1998). Telomere maintenance is dependent on activities required for end repair of double-strand breaks. *Curr. Biol.* 8, 657–660.
- Palm, W., and de Lange, T. (2008). How shelterin protects mammalian telomeres. *Annu. Rev. Genet.* 42, 301–334.
- Rog, O., Miller, K.M., Ferreira, M.G., and Cooper, J.P. (2009). Sumoylation of RecQ helicase controls the fate of dysfunctional telomeres. *Mol. Cell* 33, 559–569.
- Sfeir, A., Kosiyatrakul, S.T., Hockemeyer, D., MacRae, S.L., Karlseder, J., Schildkraut, C.L., and de Lange, T. (2009). Mammalian telomeres resemble fragile sites and require TRF1 for efficient replication. *Cell* 138, 90–103.
- Simon, M.N., Churikov, D., and Géli, V. (2016). Replication stress as a source of telomere recombination during replicative senescence in *Saccharomyces cerevisiae*. *FEMS Yeast Res* 16, fow085.
- Subramanian, L., Moser, B.A., and Nakamura, T.M. (2008). Recombination-based telomere maintenance is dependent on Tel1-MRN and Rap1 and inhibited by telomerase, Taz1, and Ku in fission yeast. *Mol. Cell Biol.* 28, 1443–1455.
- Takikawa, M., Tarumoto, Y., and Ishikawa, F. (2017). Fission yeast Stn1 is crucial for semi-conservative replication at telomeres and subtelomeres. *Nucleic Acids Res.* 45, 1255–1269.
- Teixeira-Silva, A., Ait Saada, A., Hardy, J., Iraqui, I., Nocente, M.C., Fréon, K., and Lambert, S.A.E. (2017). The end-joining factor Ku acts in the end-resection of double strand break-free arrested replication forks. *Nat. Commun.* 8, 1982.
- Vannier, J.-B., Pavicic-Kaltenbrunner, V., Petalcorin, M.I.R., Ding, H., and Boulton, S.J. (2012). RTEL1 dismantles T loops and counteracts telomeric G4-DNA to maintain telomere integrity. *Cell* 149, 795–806.
- Webb, C.J., and Zakian, V.A. (2008). Identification and characterization of the *Schizosaccharomyces pombe* TER1 telomerase RNA. *Nat. Struct. Mol. Biol.* 15, 34–42.
- Webb, C.J., and Zakian, V.A. (2012). *Schizosaccharomyces pombe* Ccq1 and TER1 bind the 14-3-3-like domain of Est1, which promotes and stabilizes telomerase-telomere association. *Genes Dev.* 26, 82–91.
- Wenz, C., Enekel, B., Amacker, M., Kelleher, C., Damm, K., and Lingner, J. (2001). Human telomerase contains two cooperating telomerase RNA molecules. *EMBO J.* 20, 3526–3534.
- Xu, Z., Fallet, E., Paoletti, C., Fehrmann, S., Charvin, G., and Teixeira, M.T. (2015). Two routes to senescence revealed by real-time analysis of telomerase-negative single lineages. *Nat. Commun.* 6, 7680.

Yamazaki, H., Tarumoto, Y., and Ishikawa, F. (2012). Tel1(ATM) and Rad3(ATR) phosphorylate the telomere protein Ccq1 to recruit telomerase and elongate telomeres in fission yeast. *Genes Dev.* 26, 241–246.

Ye, J., Lenain, C., Bauwens, S., Rizzo, A., Saint-Léger, A., Poulet, A., Benarroch, D., Magdinier, F., Morere, J., Amiard, S., et al. (2010). TRF2 and apollo cooperate with topoisomerase 2alpha to protect human telomeres from replicative damage. *Cell* 142, 230–242.

Zhu, Z., Chung, W.-H., Shim, E.Y., Lee, S.E., and Ira, G. (2008). Sgs1 helicase and two nucleases Dna2 and Exo1 resect DNA double-strand break ends. *Cell* 134, 981–994.

Zimmermann, M., Kibe, T., Kabir, S., and de Lange, T. (2014). TRF1 negotiates TTAGGG repeat-associated replication problems by recruiting the BLM helicase and the TPP1/POT1 repressor of ATR signaling. *Genes Dev.* 28, 2477–2491.

STAR★METHODS

KEY RESOURCES TABLE

REAGENT or RESOURCE	SOURCE	IDENTIFIER
Antibodies		
Anti-Rad51	abcam	ab63799; RRID: AB_1142602
Anti-HA (12CA5)	Merck	Roche Cat# 11583816001; RRID: AB_514505
Anti-Myc (c-Myc antibody; 9E10)	Santa cruz	Santa Cruz Biotechnology Cat# sc-40; RRID: AB_627268
Anti-V5	Life technologies	Thermo Fisher Scientific Cat# R960-25; RRID: AB_2556564
Chemicals, Peptides, and Recombinant Proteins		
Proteinase K	Euromedex	EU0090
RNase A DNase-free	Roche	11119915001
Lysing enzymes	Sigma	L1412
Zymolyase 100T	Amsbio	120493-1
Benzoylated Naphtoylated DEAE-cellulose (BND)	Sigma	B6385
Dynabeads protein G	Invitrogen	10003D
NEB Buffer 3.1	New England Biolabs	B7203S
CutSmart buffer	New England Biolabs	B7204S
Beta-agarase	New England Biolabs	M0392L
5-Fluoroorotic Acid (5-FoA)	Euromedex	1555
Ultra-Hyb Buffer	Invitrogen	AM8669
Glycogen	Roche	10901393001
Caffeine	Sigma	C-8960
Poly-prep Chromatography columns	Biorad	731-1550
Deoxycytidine 5'-triphosphate (α -32P)	Perkin Elmer	BLU013Z250UC
Phos-tag	Wako	ALL-107
Formaldehyde	Sigma	F-8775
Agarose ULTRAPURE	Life technologies	105001100
Agarose, low gelling temperature	Sigma	A9414
<i>Nsil</i> , recombinant	New England Biolabs	R0127L
<i>EcoRI</i> -HF	New England Biolabs	R3101S
Hybond-XL membrane	Dutsher	RPN2035
Critical Commercial Assays		
Genomic-Tip 20/G	QIAGEN	10223
TB Green premix Ex TaqII (Tli RNase H Plus)	TAKARA	RR820W
InnuPrep PCR pure Kit	AnalytikJena	845-KS-5010250
Illustra microspin	GE-healthcare	2753001
Experimental Models: Organisms/Strains		
See Table S1 a list of yeast strains used in this study		
Oligonucleotides		
See Table S2 a list of primers used in this study		
Software and Algorithms		
Quantity One 1-D analysis software	Biorad	N/A

LEAD CONTACT AND MATERIALS AVAILABILITY

Further information and requests for resources and reagents should be directed to and will be fulfilled by the Lead Contact, Stéphane Coulon (stephane.coulon@inserm.fr).

All unique/stable reagents generated in this study are available from the Lead Contact without restriction.

EXPERIMENTAL MODEL AND SUBJECT DETAILS

SchizoSaccharomyces pombe strains used in this paper are derivatives of the standard strains 972h- and are listed in [Table S1](#). Strains were grown under standard conditions in YES (Yeast Extract with Supplements) at 30°C if not indicated otherwise. Further specifications are mentioned within the Methods Details section.

METHOD DETAILS

Strains and Plasmids

S. pombe strains used in this work are listed in [Table S1](#). Telomerase was deleted by substituting the *ter1* gene by kanamycin cassette by one-step homologous insertion as described previously ([Maestroni et al., 2017a](#)). Diploid strains were sporulated and genotype was verified following the genetic markers or by PCR (see [Table S2](#)). To get rid of pREP2-Trt1 plasmid carrying the *ura4+* marker, cells were replicated on 5-Fluoroorotic acid (5-FOA) plates.

Liquid senescence assay

After micromanipulation or transformation, cells were grown in 50 mL of YES medium at 32°C and the starting OD₆₀₀ was set to 0.0013 each day. Population doublings were calculated each day as the log₂ (OD₆₀₀/0.0013), where the OD₆₀₀ is the cell density measured after 24 hr. Graphs were plotted using Prism7.

Telomere length analysis by Southern blotting

Genomic DNA was prepared from 15 mL of cells at OD_{600nm} = 1 and digested either with *ApaI* or *EcoRI*. The digested DNA was resolved in a 1.2% agarose gel and blotted onto a Hybond-XL membrane (Dutsher, RPN2035). After transfer, the membrane was cross-linked with UV and hybridized with a telomeric probe. ³²P labeling of DNA probes was performed with alpha-³²P dCTP (Perkin Elmer, BLU013Z250UC) and Illustra microspin column (GE-healthcare). The telomeric and subtelomeric STE1 DNA probes were extracted by digestion of pIRT2-Telo plasmid by *SacI*/*PstI* and *EcoRI*/*ApaI*, respectively ([Rog et al., 2009](#)). Chromosomal probes were also used as a loading control. It corresponds to a genomic region of chromosome II that could be amplified by the primers listed on [Table S2](#). These probes reveal fragments at 5 and 1.1 kb when genomic DNA is digested with *EcoRI* and *NsiI*, respectively.

Chromatin Immunoprecipitation (ChIP)

Cells (100ml at OD_{600nm} = 0.8) were resuspended in lysis buffer (50mM HEPES-KOH pH 7.5, 140 mM NaCl, 1 mM EDTA, 1% Triton X-100, 0.1% sodium deoxycholate). The crude cell lysate was sonicated to yield 0.5–1kb DNA fragments and clarified by centrifugation for 15 min at 16,000g. Prior to immunoprecipitation, 1/10 volume of the cell lysate was saved for an input control. Antibodies 9E10 anti-myc (Santa Cruz, sc40), anti-Rhp51 (Abcam, ab63799) and anti-V5 (Invitrogen, R960-25) mouse monoclonal antibodies were added to whole-cell extracts and incubated 1h at 4°C on a rotator wheel, and then magnetic Dynabeads (Invitrogen) were added for 1.5h at 4°C. Immunoprecipitates were washed three times each with 1ml of lysis buffer, 1ml of lysis buffer/500mM NaCl, two times each with 1ml of wash buffer (10mM Tris-HCl pH 8, 0.25M LiCl, 0.5% NP-40, 0.5% sodium deoxycholate, 1mM EDTA) and 1 mL of TE buffer (10mM Tris-HCl, 1mM EDTA pH 8). Recovered DNA was analyzed either by SYBR Premix Ex TaqII (Tli RNase Plus) (RR820W) using telomeric (Telo) or chromosomal (Ch) primers that are listed in [Table S2](#).

Two-dimensional (2D) gel electrophoresis

Replication intermediates (RIs) were analyzed as follows: 2.5x10⁹ cells were washed in cold SP1 buffer (1.2M sorbitol, 50mM citrate phosphate, 40mM EDTA, pH 5.6) Cells were treated with 0.625 mg/ml lysing enzyme (Sigma, L1412) and 0.5 mg/ml zymolyase 100T (Amsbio, 120493-1). The resulting spheroplasts were then embedded in low gelling temperature agarose (Sigma A9414) plugs, incubated in a digestion buffer containing proteinase K (Euromedex, EU0090) and stored in TE (50 mM Tris, 10 mM EDTA). DNA was digested with 60 units per plug of the restriction enzyme *NsiI* (NEB, R0526M) and then treated with RNase (Roche, 11119915001) and beta-agarase (NEB, M0392L). Melted Plugs were equilibrated with 0.3M NaCl and replication intermediates enrichment was achieved on BND cellulose (Sigma, B6385) embedded in columns (Biorad, 731-1550), as described ([Lambert et al., 2010](#)) or with Genomic-Tip 20/G (QIAGEN). Replication intermediates were enriched in the 1M NaCl 1.8% caffeine (Sigma, C-8960). After precipitation with glycogen (Roche, 10901393001), Replication intermediates were separated by electrophoresis in 0.4% and 1% (+ EtBr 0.5 mg/ml) agarose gels in 1X TBE for the first and second dimensions ([Brewer et al., 1992](#)). DNA was transferred to a nylon membrane (Dutsher, RPN2035) in 10X SSC. Membranes were incubated with a ³²P radio-labeled STE1 probe (Illustra microspin column, GE-healthcare and alpha-³²P dCTP, Perkin Elmer, BLU013Z250UC) in Ultra-Hyb buffer (Invitrogen, AM8669) at 42°C. Replication intermediates were detected using Biorad molecular imager Fx.

Protein extraction and western blots

Total protein extracts were prepared from 1x10⁸ cells. Cells were washed with 20% trichloroacetic acid (TCA) in order to prevent proteolysis and were resuspended in 200µl of 20% TCA at room temperature. After addition of the same volume of glass beads, cells were disrupted by FastPrep (MP Biomedical) 6.5 three times, 20sec at 4°C. Glass beads were washed twice with 200 µl of 5% TCA

acid, and the resulting extract was spun for 15min at 16,000g at 4°C. The pellet was resuspended in 200 μ l of Laemmli buffer, neutralized by adding 10 μ l of 1M Tris base, and finally clarified by centrifugation as described above. For western blots, 20 μ l of aliquots were separated in 7% polyacrylamide gels containing 25mM Phos-tag (AAL-107, NARD, Wako), transferred to a nitrocellulose filter (Amersham), and probed with mouse anti-HA 12CA5 (Roche) and mouse 9E10 anti-myc (Santa Cruz, sc40) antibodies. Immunoblots were developed using the enhanced chemiluminescence procedure (ECL kit, Perkin Elmer).

QUANTIFICATION AND STATISTICAL ANALYSIS

Statistical parameters are reported in the Figures and the Figure Legends. p values are calculated from two-tailed t test.

DATA AND CODE AVAILABILITY

All sequencing data and software used are available from the lead author, upon request.